

LAND USE DEPENDENT SNOW COVER RETRIEVAL USING MULTITEMPORAL, MULTISENSORAL SAR-IMAGES TO DRIVE OP- ERATIONAL FLOOD FORECASTING MODELS

A. Löw, R. Ludwig, W. Mauser

*Department of Earth and Environmental Sciences,
Chair of Geography and Geographical Remote Sensing, University of Munich
Luisenstrasse 37, D-80333 Munich, phone.: ++49-89-2180-6690, fax.: ++49-89-2180-6675,
eMail: a.loew@lmu.de*

ABSTRACT

The DLR-funded project “Integration of remote sensing data in operational water balance and flood forecasting systems” (InFerno⁺) has been originated to establish an operational synergy of remote sensing and flood forecasting. Upon availability, InFerno⁺ intends to make excessive use of ENVISAT ASAR data, which will provide microwave imagery at a specifically appropriate spatial and temporal resolution. New methodologies, based on existing and ongoing research initiatives for the derivation of soil moisture and snow properties, are being developed in the catchments of the Ammer, Neckar, and Mosel rivers. These are brought to an operational level, by means of algorithm retrieval and software development, to automatically process remote sensing data and to assimilate this information in the hydrological model LARSIM. In the presented study, ENVISAT performance is simulated in a multitemporal and multisensoral attempt to delineate snow cover from RADARSAT and ERS imagery. For the retrieval of snow covered area (SCA) by means of SAR, image rationing has been established as the state-of-art method. It derives information on the areal extent of wet SCA, which, due to its critical energetic stage, is a tremendously important indicator for flood risk. To obtain areal maps of SCA, a landuse-dependent thresholding for the difference between the reference and the data take of interest is applied. For crop fields a threshold of -4 dB, for pasture a threshold of -2 dB is determined. The snow line obtained from SAR imagery is validated by point observations of the German Weather Service (DWD). Analyses show, that SAR imagery, presuming high spatial and temporal resolution, provides most promising results in terms of SCA detection.

INTRODUCTION

The potential of remote sensing data has gained increasing consideration in numerous hydrological applications (3-5). The possibility to image spatial characteristics and to retrieve manifold quantitative information over large areas has been recognised as a useful tool in complex water-related issues, such as water balance modelling or yield estimation. However, due to the coarse temporal resolution of available spaceborne imagery, the utilisation of remote sensing is yet uncommon in the field of operational flood forecasting and flood management, where information on soil and snow properties, as fundamental flood-steering parameters, needs to be provided at high temporal frequency.

Methods to accurately assess and forecast flood discharge are a fundamental requirement in practical hydrology. Existing rainfall-runoff models seldom consider the spatial characterisation of the land surface. In order to obtain reliable flood predictions, an accurate physically based description of the processes contributing to runoff formation is essential. The new generation of remote sensing systems, such as ENVISAT, will deliver relevant spatial model input parameters at a sufficient temporal frequency to gather the information required for trustworthy flood forecasting.

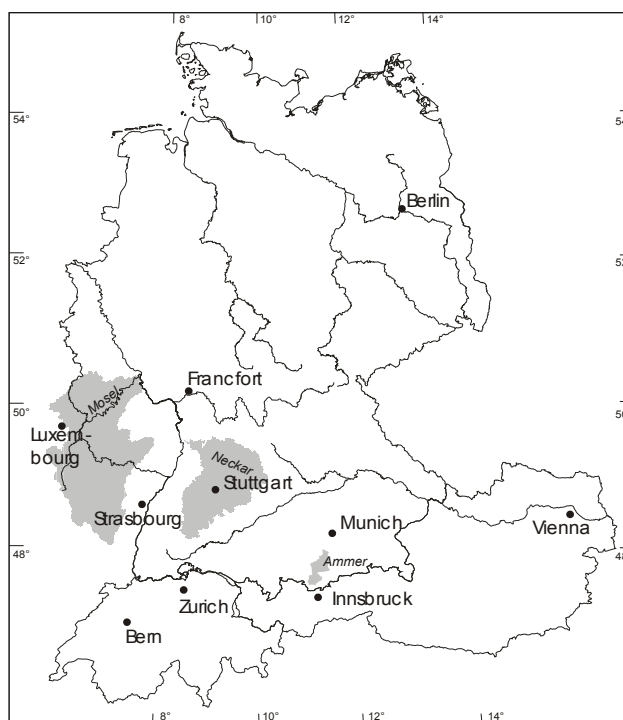


Figure 1: *InFerno+ Testsites*

The objective of the DLR funded project *InFerno+* (1) is to improve spatial input parameters for an operational flood forecasting model and to assimilate remote sensing information in the water balance and flood forecasting system LARSIM (2). A usage of ENVISAT ASAR data in synergy with optical imagery has a strong potential to make model parameterisation independently feasible, and hence regionally transferable.

Scientific work is performed in the catchments of the Ammer (~ 700 km²) and Neckar (~ 14.000 km²) rivers. In a later stage, the developed algorithms and methods are transferred to the binational Mosel watershed (~ 28.000 km²) to evaluate their regionalized applicability (Fig. 1).

Floods in the test areas are mainly caused by two factors: heavy rain and rain in combination with snow melt. For the Neckar and Mosel catchments, two federal Flood Forecasting Centres have been established to predict the water levels for more than 40 gauges in the catchments. The forecast is currently based on the use of gauge observations and meteorological recordings. Reliable information on soil moisture conditions and snow properties, such as snow wetness, snow water equivalent and snow covered area (SCA), are believed to significantly improve the current quality and reliability of forecasts.

The importance of microwave remote sensing to derive parameters for hydrologic applications has been impressively shown in numerous studies (3-5). With the use of microwave data it is e.g. possible to derive soil moisture information (6) or snow properties (5,13,14). Optical sensors have also shown their principal capability for mapping SCA (7,8) and for measuring certain snow properties, but suffer from the drawback, that cloudy conditions prevent any kind of utilizable observations.

Numerous investigations have been carried out to examine the capabilities of microwave sensors for mapping snow properties. It has been shown that dry snow is almost transparent in the microwave region of the electromagnetic spectrum (9,10). As opposed to this, wet snow with a liquid water content of even less than 1% has considerable influence on the permittivity of the snowpack. Increasing absorption results in a significant reduction of the backscattering coefficient (11,27). Table 1 lists measured values of snow properties reported in (13).

Table 1: Dielectric properties of dry and wet snow (13)

Medium	Dielectric constant ϵ'	Dielectric constant ϵ''	Penetration depth L_p [m]	Snow density ρ [g cm ⁻³]	Content of free water W [%]
Water	66	36	-	-	-
Ice	3.1	8E-10	65	-	0
Snow (dry)	1.6	4E-4	60	0.35	9
Snow (wet)	1.9	0.08	0.3	0.35	3
Snow (wet)	2.2	0.15	0.18	0.35	5
Snow (wet)	2.6	0.28	0.1	0.35	8

The significant contrast between wet and dry snow enables wet snow-covered areas to be delineated using a snow-free or dry snow-covered reference image and the corresponding wet snow image. In order to minimize terrain-dependent backscatter changes, repeat pass images have to be used. Wet snow is classified by rationing the two calibrated images and applying an empirical threshold to that ratio image (Fig. 2).

$$\text{Ratio} = 10 \times \log \left(\frac{\text{Snow}}{\text{Reference}} \right)$$

Figure 2: Ratio method for wet snow cover mapping

It was found that a threshold of ~ -3 dB is applicable to delineate the wet snow extent (12-14) for ERS data. For RADARSAT data, (16) found no significant backscatter differences between dry and wet snow conditions. The difference between the snow and reference image depends on the land use and the incidence angle (15,16). A slightly different approach was proposed by (17), where three images were used to derive subscale wet snow cover, one from the starting melting season, one during the melting season, and one snow free reference image.

The snow mapping algorithms have shown their capability for improving runoff forecasting for alpine catchments (18). The transparency of dry snow cover in C-band makes it impossible to map snow-covered areas under dry snow conditions. However, the snow water equivalent (SWE) and the snow melt probability are of major interest for hydrologic applications. While melting snow can be detected with sufficient accuracy from single frequency, single polarization measurements, the retrieval of SWE requires parameterization from multifrequency polarimetric SAR systems and is limited to certain surface conditions (19,20).

ENVISAT ASAR will provide different acquisition modes, which will allow for multiple data takes of the same area within a few days (32). To benefit from this high temporal frequency, robust algorithms have to be established, taking changes into account which are induced by varying incidence angles and land use effects. Until ENVISAT data is available, InFerno⁺ will develop algorithms and methods to derive snow parameters from existing sensors like ERS and RADARSAT, which are applicable to simulate the different acquisition modes of ASAR.

A case study is carried out, using data from February 1999, to demonstrate the potential of different acquisition modes for snow mapping in the InFerno⁺ areas. This paper presents first results using a multitemporal, multisensoral approach for snow delineation using ERS and RADARSAT ScanSAR data. Additional investigations in the Ammer catchment area are shown, analyzing the influence of heterogeneous land use for the rationing method.

SAR DATA SET

The available SAR data for the Neckar catchment consists of a pair of snow-covered RADARSAT and ERS images taken in February 1999 and corresponding snow-free reference scenes. Between the two sensor overflights, the snow cover patterns changed rapidly. The Ammer test site dataset covers the winter seasons since 1995/96. Investigations are focussed on a small number of selected scenes with varying snow conditions (Table 2). Snow parameters were measured during accompanying field campaigns in the winters of 1999 and 2000.

Table 2a: SAR Dataset Ammer Testsite

Date	Sensor	Format/Mode	Snow conditions	Field data
15.02.1996	ERS	SLC	Wet snow	-
04.02.1999	ERS	SLC	Wet snow	x
10.03.1999	ERS	SLC	Melting, almost snow free	x
11.03.1999	ERS	SLC	Melting, almost snow free	x
20.01.2000	ERS	SLC	Wet snow	-
06.03.1999	ERS	SLC	Reference scene, snow free	-
20.01.2000	ERS	SLC	Wet snow	-

Table 2b: SAR Dataset Neckar Testsite

Date	Sensor	Format/Mode	Snow conditions
6.4.1998	RADARSAT	ScanSAR Narrow	Snow free
22.02.1999	RADARSAT	ScanSAR Narrow	Wet snow, melting phase
13.11.1998	ERS	SLC	Snow free
26.02.1999	ERS	SLC	Wet snow, melting phase

In contrast to RADARSAT standard images (28), the potential of ScanSAR mode for snow mapping has not been intensively investigated yet. First results were presented by (25) for the Swiss Alps. Despite the lower radiometric and geometric accuracies of the ScanSAR products, snow cover was mapped with good results.

For the different sensors and products, the processing chain has to be slightly adjusted. The main processing steps consist of calibration, filtering, and geocoding of the datasets (Fig. 3).

For ERS SLC data, calibration is performed using the method of (21). The RADARSAT digital numbers are converted to backscattering coefficients by inverting the processor output scaling look up table, using the algorithm of (22).

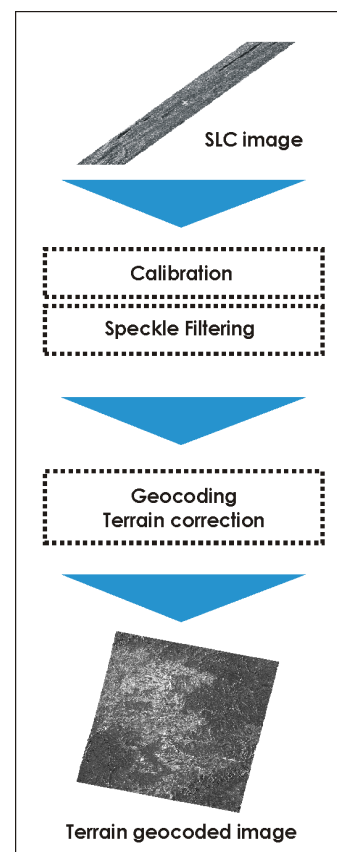


Figure 3: SAR processing chain

Geocoding

The use of two different sensors and different products requires adapted geocoding procedures. The geocoding of the ERS SLC data was performed using the algorithm of (24). It implies geometric and radiometric correction of the data using a digital elevation model (DEM). The images were geocoded to UTM projection with 100 m resolution. Terrain-induced backscatter deviations are diminished using a maximum entropy preserving approach.

The RADARSAT ScanSAR product, delivered by the Canadian Data Processing Facility (CDPF), is an ellipsoid geocoded product with a nominal pixel spacing of 25 m (ScanSAR Narrow – SCN) or 50 m (ScanSAR wide – SCW). Therefore the geocoding procedure of (24) cannot be applied to this data. It was decided to apply a second order polynomial rectification to a landuse map of the area of interest using selected ground control points (GCP). The accuracy of rectification depends on the topography. For flat terrain, the error was less than one pixel. For rugged terrain the relief-induced distortions, which are not taken into account in the ellipsoid geocoded product, result in errors of a few pixels. A map of incidence angles was calculated for both sensors.

Filtering

The separation of snow-covered and snow-free areas requires a high radiometric accuracy. The SAR-immanent speckle leads to considerable variances in image statistics. The probability of error for the presented snow mapping algorithm depends on the efficient number of looks in the image and the desired threshold, which is to be applied for snow cover mapping. An efficient number of looks greater than 64 is needed to apply a threshold of ~ 2.5 dB on the level of significance of 95 % (23).

A high number of looks can be obtained by averaging several statistically independent samples, such as adjacent pixels, or by applying speckle filters. Intensive tests on filtering and geocoding ERS data were carried out to find best radiometric accuracies preserving spatial resolution. It was found that the Frost speckle filter (26), with a window size of 9x9 pixels, provides best results in geocoding an image to a DEM with 30 m resolution. However, speckle filtering has no effect, when geocoding the image to a DEM with 100 m resolution. The maximum entropy-preserving approach of (24) leads to an efficient number of looks greater than 80. This is sufficient to distinguish classes with a class difference of ~ 2 dB on the 95 %-level of significance. The investigations discussed in the next section are carried out for data geocoded on 100 m resolution DEMs.

LAND USE DEPENDENCY

The snow mapping algorithm is mainly based on the assumption, that the surface conditions of the reference scene are homogeneous. To reduce the effect of different moisture and soil conditions and speckle, (33) propose to use a multitemporal average of different reference scenes for detection. This was not yet possible in our investigation, because two of the three snowfree scenes available (Table 2a) were acquired after a melting period. We therefore decided to use only one scene as reference.

Due to significant differences in surface roughness, harvested crop fields have higher backscatter coefficients than grassland. Assuming comparable snow conditions, the difference between the reference and the snow scene is consequently higher for crop fields. To investigate the different behaviour of backscatter difference $\Delta\sigma$, ratio images were calculated and the image statistics were analysed for selected test areas within the pre-alpine Ammer test site. Figure 4 shows the selected sub-regions, each characterized by different predominant land-use distributions.

For each region, the mean land use-specific backscatter difference was calculated (Fig. 5). It can be seen that, depending on the snow conditions, the backscatter difference can be either positive or negative. The images with wet snow conditions (Feb. 1996, 1999 and Jan. 2000) show a significant

reduction of backscatter. On March 10th and 11th 1999 (free of snow following a melting period), saturated soils lead to increasing backscatter values .

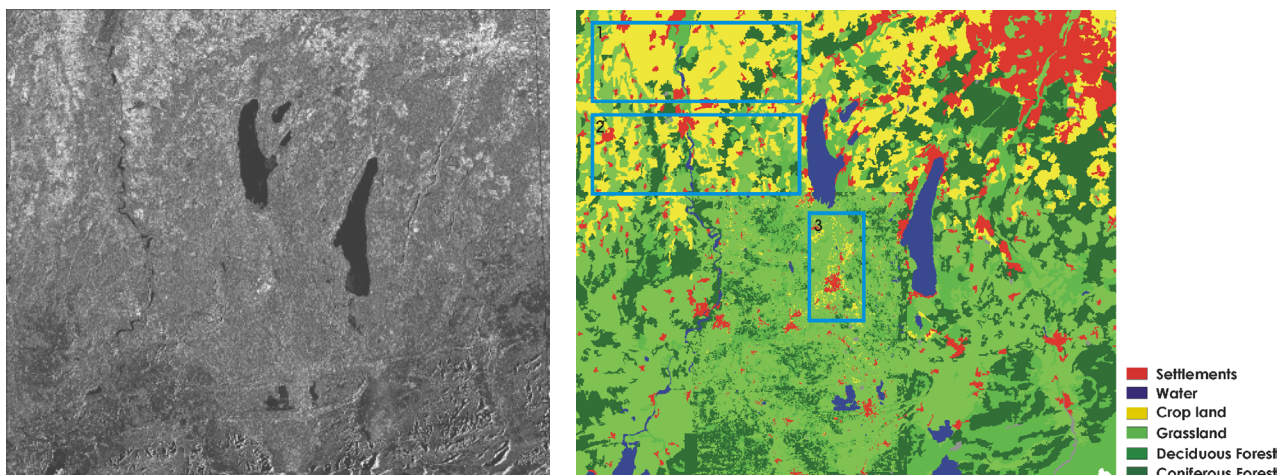


Figure 4: Ammer test site: ERS Reference image 6.3.1997 and landuse map

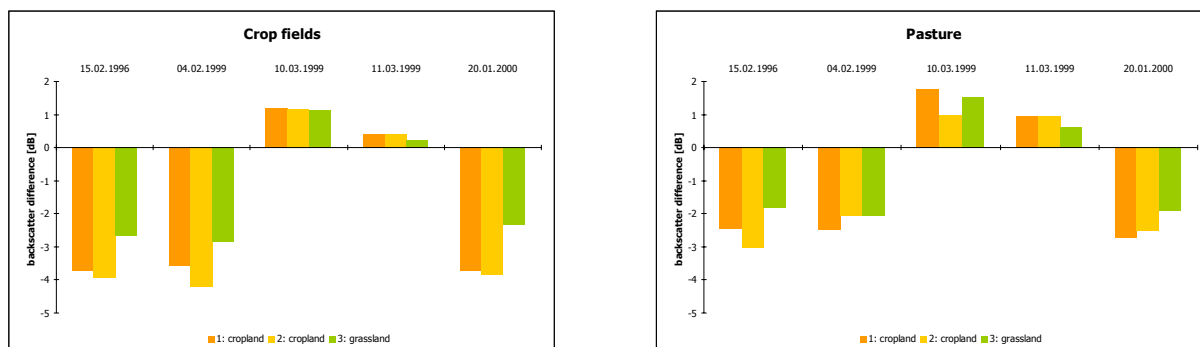


Figure 5: Backscatter changes for crop fields and pasture for the three subregions

The difference for crop is about 2 dB larger (~ 4 dB instead of ~ 2 dB than for grassland), except for areas where grassland dominates. There, $\Delta\sigma$ for the cropfields is only slightly higher than for grassland. This can be explained by mixed pixels of crop and grassland, which increase attenuation in the reference image and consequently reduce $\Delta\sigma$.

As discussed above, the probability of classification error strongly depends on the applied threshold. To map the SCA, it is suitable to (A) apply a small threshold as -2 dB to obtain spatially distributed snow cover maps or (B) apply a greater threshold as e.g. -4 dB to derive a smaller number of snow-covered pixels with a high contrast resulting in a higher classification accuracy. It depends on the purpose of data assimilation into a flood forecasting model, to judge the appropriate procedure. Classifying the images, using thresholds of -4 and -2 dB respectively, resulted in (Fig. 6).

It can be seen that a threshold of -4 dB only classifies snow on crop land, whereas a threshold of -2 dB classifies almost the whole test area as snow. Comparisons with field observations and measurements of the German Weather Service (DWD) show good correspondence with the SCA map obtained by thresholding at -2 dB.

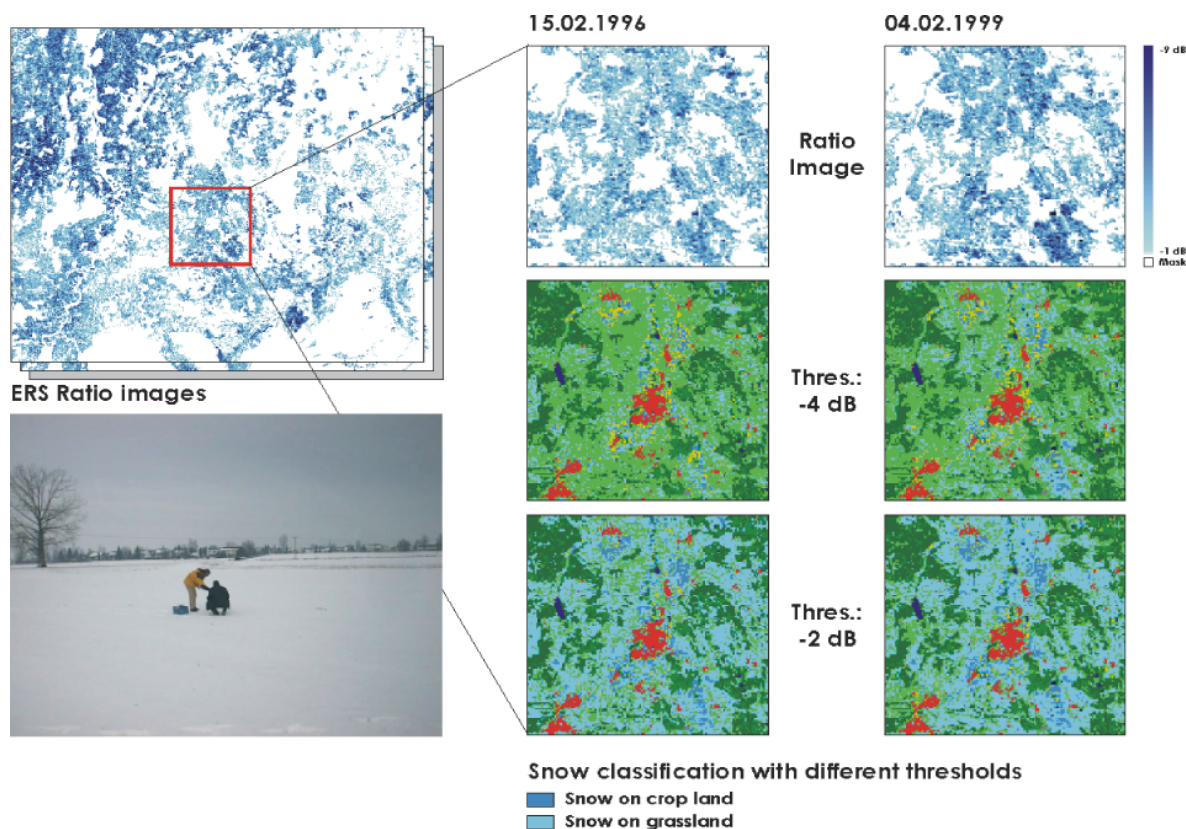


Figure 6: Snow classification results using different thresholds. Classification is only performed in open areas and not in forests or settlements. Measurements on 3.2.1999.

MULTITEMPORAL, MULTISENSORAL SNOW COVER ESTIMATION

Two RADARSAT ScanSAR Narrow Mode images from Feb. 22nd 1999 and April 6th 1998 cover the southern part of the German midlands including the Black Forest and the Central and Eastern alps. The part containing the Neckar test site in southwestern Germany was rectified to Gauss Krüger Projection (Central Meridian 9°) by using the GCP approach. Figure 7 shows the complete image of Feb. 22nd 1999 and the selected parts of the reference and snow image.

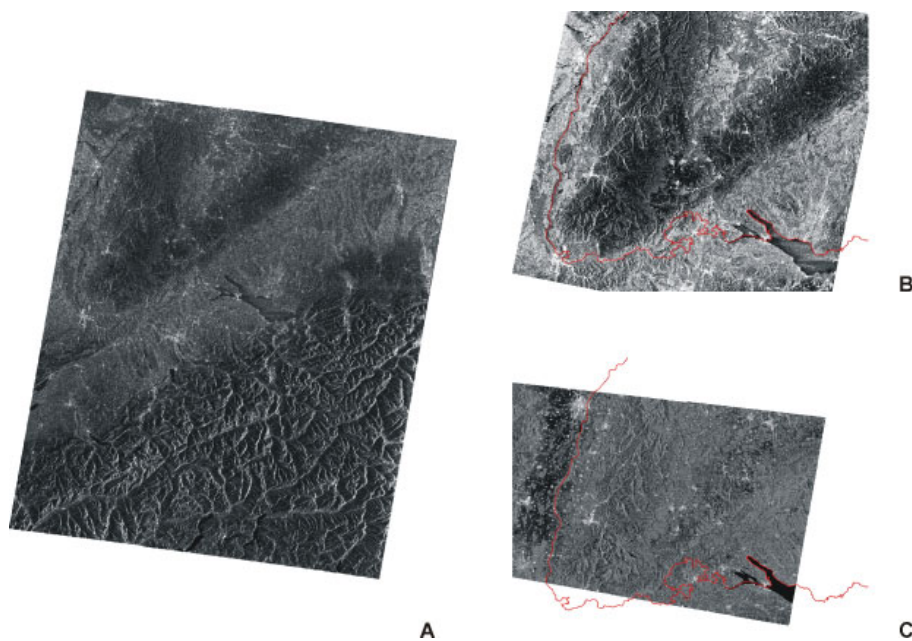


Figure 7: RADARSAT ScanSAR image 22.2.1999 (a), and parts of the snow and reference image used for snow delineation (B,C). © RADARSAT International

A corresponding ERS image was recorded on Feb. 26th 1999 (which is referred to a snow-free image from Nov. 13th 1998). Both images are terrain geocoded and terrain corrected using the procedure of (24). Additional land use information was available on a 30 m grid, taken from a landuse map distinguishing 13 different land-use classes in the test site (Fig. 9).

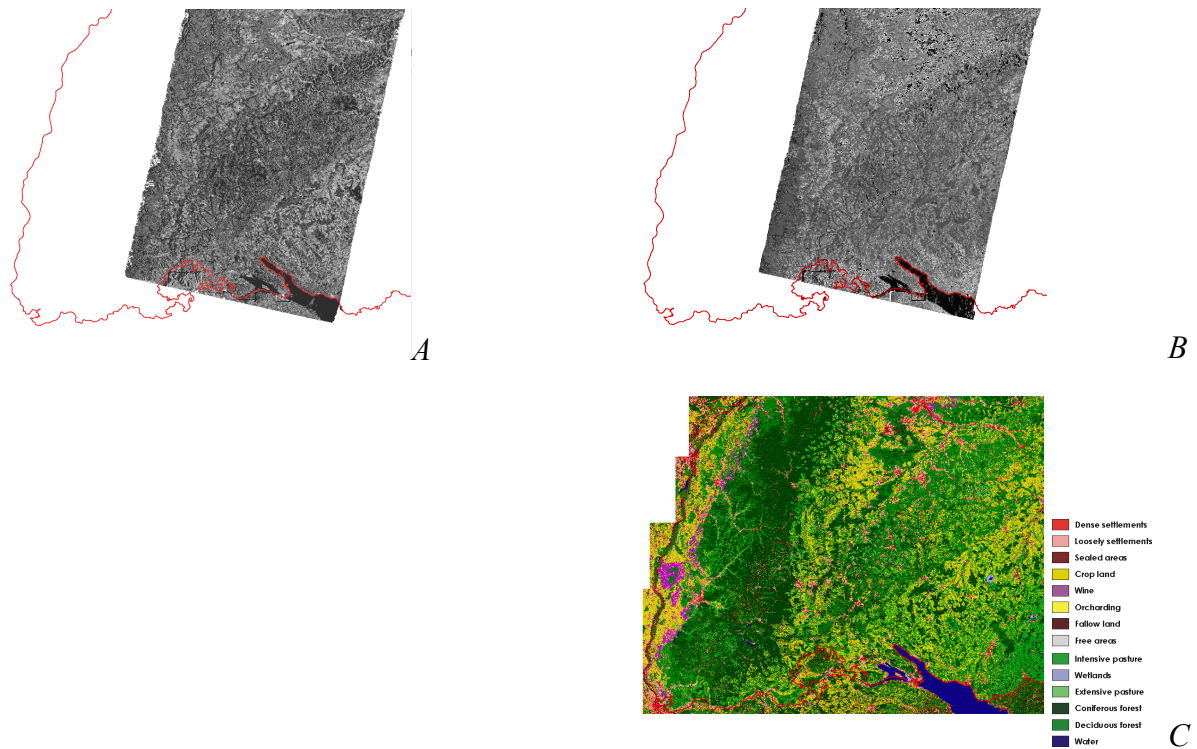


Figure 8: ERS images: Reference 13.11.1998 (A), snow image 26.02.1999 (B) and land use map

Incidence angle effects

Literature reports that the incidence angle has a significant influence on the backscattering coefficient of snow cover (11,16,29). The incidence angle for the RADARSAT image of 22.2.1999 ranges from 18° to 37°. The snow-covered parts of the image range from ~18° to 34°. To evaluate the effect of the incidence angle, polygons for 64 snow-covered areas were taken from the image to determine an eventual dependency of the backscattering coefficient. Results are shown in Figure 9. It can be seen that backscattering does not show significant dependence on the incidence angle. The reasons for this unexpected result are still matter of research and can as yet not be explained.

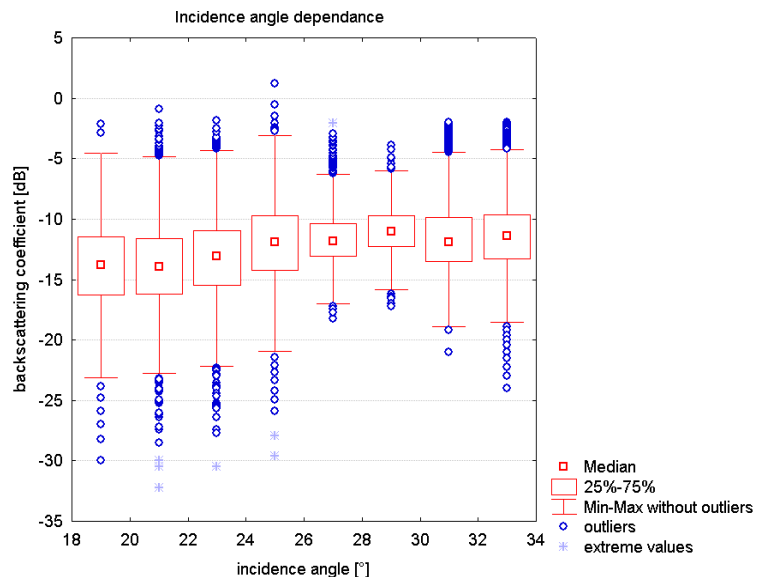


Figure 9: Incidence angle dependence of the backscattering coefficient for RADARSAT ScanSAR 22.2.1999

Snow cover estimation

The ratio between the reference and snow images was calculated for the RADARSAT and ERS data and a threshold of -2 dB was applied. The resulting snow maps are shown in figure 10. Snow can be clearly detected in open areas such as arable land, grassland, and clearings. In forested areas only a few pixels reply to the threshold criterion, thus confirming that snow cover mapping is not possible in forested areas without using a specific forest backscattering model (30).

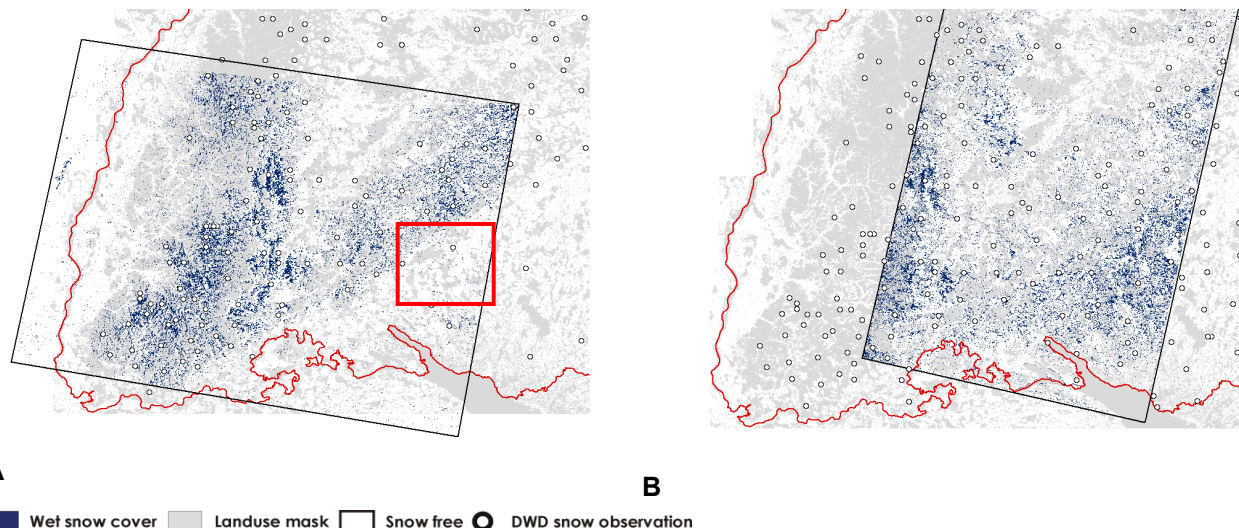


Figure 10: RADARSAT (A) and ERS (B) snow classification results based on a threshold of -2 dB

Snow conditions

The snow conditions changed rapidly between the RADARSAT and ERS image acquisition. From Feb. 18th – 22nd 1999, the snow was melting and reached a minimum on the 22nd of February. According to field observations, the lower altitudes of mountainous areas were already snow-free. Again, snowfall was observed in the southeastern part of the test site on the 23rd and 24th of February 1999. Figure 11 shows the changing snow depth recorded at three DWD stations in the area marked in Figure 10.

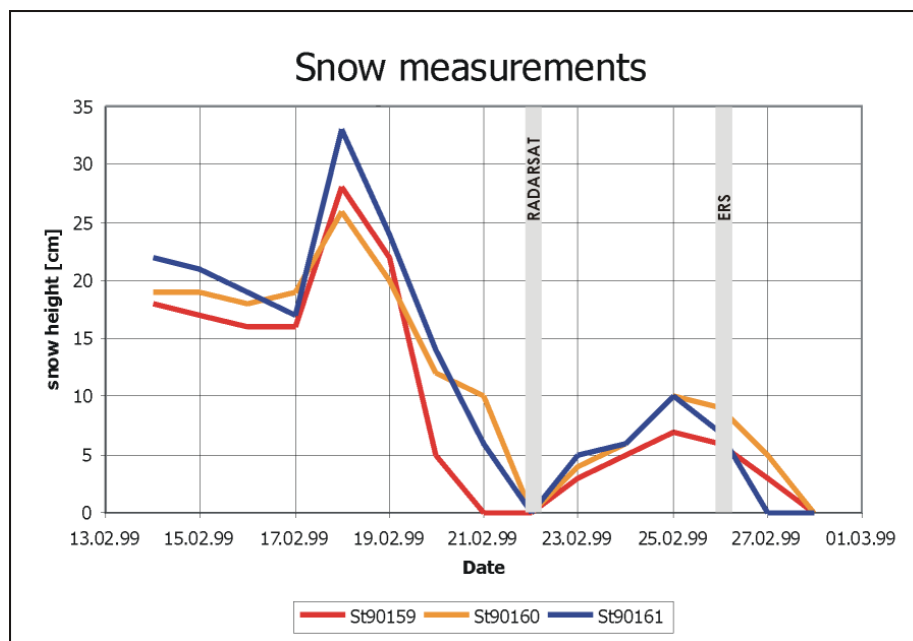


Figure 11: Observed snow depth during SAR acquisition for the area marked by the red line in Figure 10

Validation

The retrieved SCA was compared with measurements of the German Weather Service (DWD). The circles in Figure 10 show the DWD locations of observed snow packs on the day of data acquisition. The highly dynamic snow cover in the low mountain ranges is well reproduced by the remote sensing products. The evolution of SCA in the south eastern part of the test site, illustrated in Figure 11, can be detected in the classified image products.

CONCLUSIONS

The backscatter differences found for crop and pasture correspond well with previous investigations. For alpine areas and arable land, thresholds of -3 dB were found to be well suited (12-14). For heather, (31) reported a threshold of -2 dB, which is confirmed by the presented study. For SCA mapping in agricultural areas a threshold of -2 dB supplies best results. High radiometric calibration is needed to obtain products with a high level of accuracy. It can be stated that SAR-dependent snow cover mapping shows great application potential for agricultural land for model assimilation purposes. Even higher backscatter differences of ~ -4 dB provide snow classifications of utmost confidence. It has to be individually decided, which method serves the user's requirements best. The remote sensing products can hence be used to validate model results and will be capable, upon assimilation, of determining the degree of model parameter adjustment.

The high potential of snow cover mapping using different sensors and different imaging modes has been shown using ERS and RADARSAT ScanSAR data. The obtained results show good agreement with snow measurements of the German Weather Service (DWD). A threshold of -2 dB was found to provide best results.

Further research is necessary to determine the importance of incidence angle deviations for snow cover mapping. A software for terrain geocoding and terrain correction of RADARSAT ScanSAR data is under development and will be adapted to ENVISAT ASAR data to enhance the quality of the image products.

ACKNOWLEDGEMENTS

InFerno⁺ is funded by the German Aerospace Center DLR (Kz: 50EE0053). The valuable contributions of our project partners, the Flood Forecasting Centre (HVZ Karlsruhe) of the Environmental Protection Agency Baden-Württemberg, the Water Survey of Rheinland-Pfalz and VISTA GmbH (Munich), are gratefully acknowledged. Meteorological data was generously supplied by the German Weather Service DWD. ERS SAR data was provided by ESA.

REFERENCES

1. Schulz, W. *et al.* 2002. InFerno – Integration of remote sensing data in operational water balance and flood prediction modelling. Proceedings of the International Conference on Flood Estimation. Berne, Switzerland.
2. Bremicker M. 2000. Das Wasserhaushaltsmodell LARSIM - Modellgrundlagen und Anwendungsbeispiele. Freiburger Schriften zur Hydrologie. Band 11, Institut für Hydrologie, University of Freiburg
3. Strasser G. 2000. Bestimmung von hydrologischen Modellparametern aus ERS.SAR-Daten. PhD Thesis. University of Munich. 1-129.
4. Bach H. *et al.* 2000. Application of SAR-data for flood modelling in Southern Germany. Proceedings of ERS-ENVISAT-Symposium Gothenburg 2000, Looking down to Earth in the New Millennium. ESA SP-461: 123.

5. Nagler, T., Quegan, S. and Rott H. 2000. Real Time Snowmelt Runoff Forecasting using ERS SAR PRI data. Proceedings of ERS-ENVISAT Symposium, Göteborg. CD-ROM.
6. Rombach M. and Mauser W. 1997. Multi-Annual Analysis of ERS Surface Soil Moisture Measurements of Different Land Uses. Proceedings of the 3rd ERS Symposium: Space at the Service of Our Environment, ESA-SP-414. Vol 1. 27-34., Florence.
7. Derrien M. *et al.* 1993. Automatic cloud detection applied to NOAA-11 AVHRR imagery. *Remote Sens. Environ.* (46): 246-267.
8. Dozier J. 1989. Spectral signature of alpine snow cover from Landsat Thematic Mapper. *Remote Sens. Environ.* (28) : 963-969.
9. Mätzler C. 1996. Microwave Permittivity of Dry Snow. *IEEE Trans. Geosci. Remote Sensing.* 34(2): 573-581.
10. Rott H. and Mätzler C. 1987. Possibilities and Limits of Synthetic Aperture Radar for Snow and Glacier Surveying. *Annal. Glaciology.* 9: 195-199.
11. Mätzler C. 1987. Applications of the Interaction of Microwaves with the Natural Snow Cover. *Remote Sens. Reviews.* (2): 259-387.
12. Nagler T. 1996. Methods and Analysis of Synthetic Aperture Radar Data from ERS-1 and X-SAR for Snow and Glacier Applications. PhD Thesis. University of Innsbruck. 1-183.
13. Guneriussen T., Johnsen, H. and Sand, K. 1997. DEM corrected ERS-1 SAR data for snow monitoring. *Int. J. Remote Sensing.* 17(1): 181-195.
14. Baghdadi N., Gauthier Y., Bernier, M. 1997. Capability of Multitemporal ERS-1 SAR Data for Wet Snow Mapping. *Remote Sens. Environ.* 60: 174-186.
15. Rees W.G. and Steel A.M. 2001. Radar backscatter coefficients and snow detectability for upland terrain in Scotland. *Int. J. Remote Sensing.* 22(15): 3015-3026.
16. Baghdadi N. *et al.* 2000. Potential and Limitations of RADARSAT SAR Data for Wet Snow Monitoring. *IEEE Trans. Geosci. Remote Sensing.* 38(1): 316-320.
17. Koskinen J.T., Pulliainen J.T. and Hallikainen M.T. 1997. The Use of ERS-1 SAR Data in Snow Melt Monitoring. *IEEE Trans. Geosci. Remote Sensing.* 35(3): 601-610.
18. Rott H. *et al.* 2000. Hydalp - Hydrology of Alpine and High Latitude Basins: Final Report.
19. Shi J. and Dozier J. 2000. Estimation of Snow Water Equivalence Using Sir-C/X-SAR, Part I: Inferring Snow Density and Subsurface Properties. *IEEE Trans. Geosci. Remote Sensing.* 38(6): 2465-2474.
20. Shi J. and Dozier J. 2000. Estimation of Snow Water Equivalence Using Sir-C/X-SAR, Part II: Inferring Snow Depth and Particle Size. *IEEE Trans. Geosci. Remote Sensing.* 38(6): 2475-2488.
21. Laur H. *et al.* 1998. Derivation of the backscattering coefficient σ_0 in ESA SAR PRI products. ESA publication. ES-TN-RS-PM-HL09.
22. Srivastava S. 2000. Extraction of Beta Nought and Sigma Nought from RADARSAT CDPF Products. Report No.: AS97-5001. Altrix Systems.
23. Rignot E. and van Zyl, J. 1993. Change detection techniques for ERS-1 SAR data. *IEEE Trans. Geosci. Remote Sensing.* 31(4): 896-906.
24. Riegler G. and Mauser W. 1998. Geometric and radiometric terrain correction of ERS SAR data for applications in hydrologic modelling. Proceedings of IGARSS '98. 2603-2605. Seattle.
25. Haefner H., Small D., Biegger, S., Hoffmann, H. and Nüesch, D. 2001. Small-Scale Monitoring of Wet Snow Cover with RADARSAT ScanSAR data. EARSeL eProceedings No. 1, 339-346.

26. Frost V.S., Stiles J.A., Shanmugan K.S., Holtzman J.C. 1982. A Model for Radar Images and its Application to Adaptive Digital Filtering of Multiplicative Noise. *IEEE Trans. PAMI.* 4(2): 157-166.
28. Hallikainen M.T., Ulaby F.T. and Abdelrazik M. 1986. Dielectric properties of Snow in the 3 to 37 GHz Range. *IEEE Trans. Antennas and Prop.* AP-34(11): 1321-1339
29. RADARSAT International (RSI). 1999. RADARSAT User Guide. 4/99.
30. Baghdadi N., Fortin J.-P. and Bernier M. 1999. Accuracy of wet snow mapping using simulated RADARSAT backscattering coefficients from observed snow cover characteristics. *Int. J. Remote Sensing.* 20(10): 2049-2068.
31. Koskinen J. 2001. Snow monitoring using microwave radars. HUT Report 44. 1-31. Helsinki.
32. Rees W.G. and Steel A.M. 2001. Radar backscatter coefficients and snow detectability for up-land terrain in Scotland. *Int. J. Remote Sensing.* 22(15): 3015-3026.
33. ESA 1998. ENVISAT Mission & System Summary.
34. Nagler T. and Rott H. 2000. Retrieval of wet snow by means of multitemporal SAR data. *IEEE Trans. Geosci. Remote Sensing.* 38(2): 754-765.